SCIENTIFIC REPORTS

OPEN

SUBJECT AREAS:
GENETIC VECTORS
VIRAL VECTORS

Received
17 June 2014

Accepted
30 September 2014

Published
22 October 2014

Correspondence and requests for materials should be addressed to G.P.K. (gary.kobinger@phac-aspc.gc.ca)

Novel Adeno-associated Viruses Derived From Pig Tissues Transduce Most Major Organs in Mice

Alexander Bello[1,2], Allan Chand[1,2], Jenna Aviles[1,3], Geoff Soule[1], Alberto Auricchio[4,5] & Gary P. Kobinger[1,2,3]

[1]Public Health Agency of Canada, National Microbiology Laboratory, Special Pathogens Program, Winnipeg, Canada, [2]University of Manitoba, Department of Medical Microbiology, [3]Department of Immunology, Winnipeg, Canada, [4]Telethon Institute of Genetics and Medicine, Naples, Italy, [5]Medical Genetics, Translational Medicine, ''Federico II'' University, Naples, Italy.

Recently, development of Adeno-associated virus (AAV) vectors has been focusing on expanding the genetic diversity of vectors from existing sequences via directed evolution or epitope remapping. Apart from intelligent design, AAV isolation from natural sources remains an important source of new AAVs with unique biological features. In this study, several new AAV sequences were isolated from porcine tissues (AAVpo2.1, -po4, -po5, and -po6), which aligned in divergent new clades. Viral particles generated from these sequences displayed tissue tropism and transduction efficiency profile specific to each porcine-derived AAV. When delivered systemically, AAVpo2.1 targeted the heart, kidney, and muscle, AAVpo5 performed poorly but was able to transduce muscle fibers when injected intramuscularly, whereas AAVpo4 and -po6 efficiently transduced all the major organs sampled, contending with 'gold-standard' AAVs. When delivered systemically, AAVpo4 and -po6 were detected by polymerase chain reaction (PCR) and histochemical staining of the transgene product in adult mouse brain, suggesting that these vectors can pass through the blood-brain barrier with efficiencies that may be useful for the development of therapeutic approaches. Porcine tissues are antigenically similar to human tissues and by inference, porcine AAVs may provide fresh tools to contribute to the development of gene therapy-based solutions to human diseases.

Since the first account of naked DNA delivery to mammalian tissues[1], numerous methods for gene therapy have been established including gene gun, electroporation, sonoporation, viral vectors, etc.[2–5]. A good gene therapy vector should be designed to target specific tissues for a particular application and have low immunogenicity. Among these gene transfer methods being examined for *in vivo* delivery, viral vectors derived from Adeno-associated virus (AAV) have shown promising results[6–8]. The development of these vectors for gene therapy applications is attributed largely to their lack of pathogenicity, low immunogenicity, ability to establish stable long-term transgene expression in both dividing and post-mitotic cells, as well as their ability to target specific tissues[9–11]. For example, AAV1, AAV8 and AAV9 target muscle, liver and brain tissue, respectively, more efficiently than most other serotypes[12–14]. AAV serotypes with more pronounced tropisms would help to optimize therapeutic dosing in addition to decreasing the undesirable side-effects associated with non-specific transduction.

Major constraints associated with recombinant AAV (rAAV) vectors are: their limited packaging size (up to 5 Kb), the high number of genome copies required for transduction, and the possible presence of pre-existing immunity against the vector capsid, thus complicating vector administration[15,16]. Many labs have come up with novel ways to overcome the limited packaging size of AAV such as Oligo-Assisted AAV Genome Recombination (OAGR) or the creation of mini-genes, such the mini-Dystrophin gene[17,18]. AAVs are naturally present in humans and a majority of the population have pre-existing immunity towards several human AAV serotypes including AAV2 and AAV5[16,19]. In order to overcome pre-existing immunity, modification of the AAV capsid surface has been explored to prevent recognition by the host immune system. Such modifications include PEGylation of capsid surfaces or single amino-acid mutations[20,21]. To modify tissue tropisms, increase transduction efficiency and circumvent pre-existing immunity, intelligent design making use of random peptide libraries on the surface of AAV, directed evolution by shuffling AAV genomes, or creation of tyrosine-mutants have been used to enhance transduction efficiencies or modify tissue tropisms of designer AAVs[22–26]. However, although tailor-made AAVs have gained considerable popularity over the last few years, intelligent design is often limited to the utilization of traits exhibited by existing AAVs.

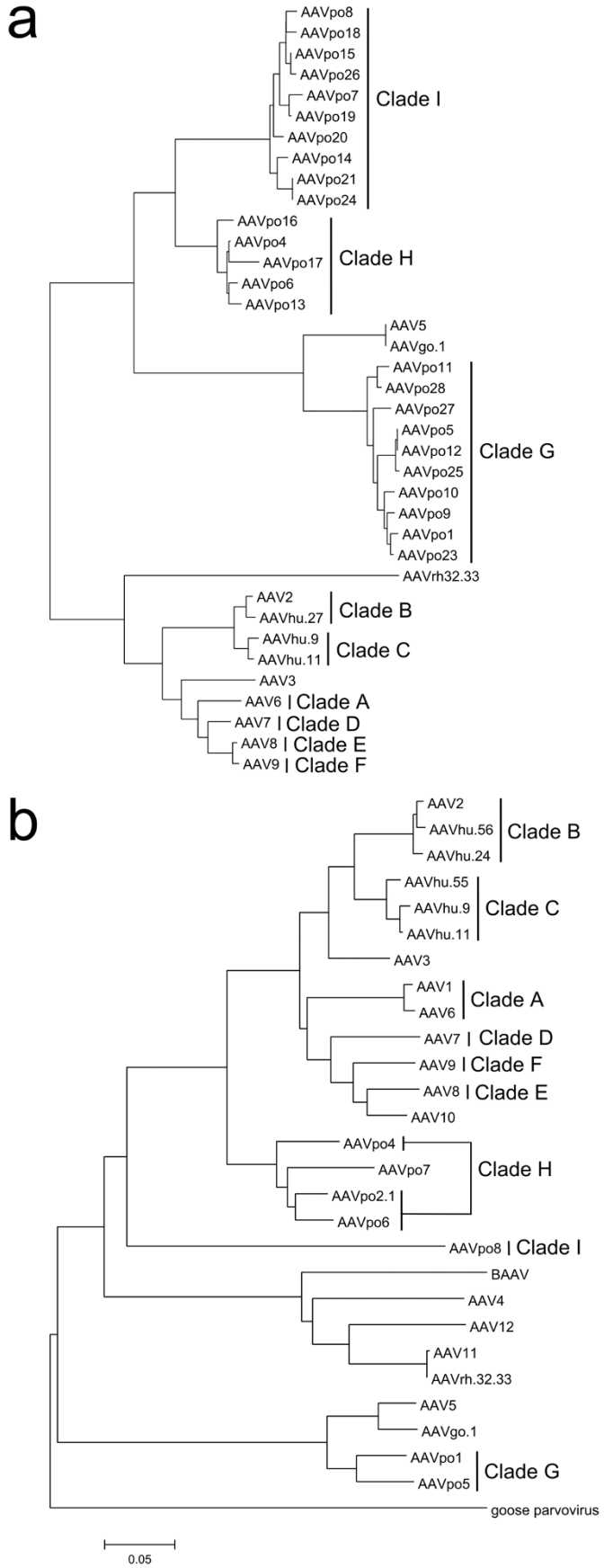

Figure 1 | Porcine-derived AAVs form several new clades within the Adeno-associated virus species. Amino acid sequence of porcine AAVs were aligned with other published AAV sequences using MUSCLE and Phylogenetic trees were inferred using the neighbor-joining method. (a) Partial sequence (~800 bp) of the beginning portion of *cap* was isolated from pig tissues and sequenced. The translated aa sequences were aligned with the same corresponding region of published AAV *cap* sequences. (b) The complete *cap* (~2.2 kb) of porcine-derived AAVs representing new clades were isolated by PCR and sequenced, and an alignment was performed with the published full-length *cap* of other AAVs. Clades are indicated by a vertical line and named in the sequential order they were identified. Figures were manipulated using Inkscape.

In addition to intelligent design, identification of novel animal AAV has been performed to identify vectors, which can improve upon current AAV properties. More than a hundred new AAV serotypes from non-human primates were isolated[27], with cross-neutralizing antibodies towards several of these novel AAVs detected in up to 30% of the human population[16]. AAVs isolated from other natural sources have not been extensively studied, with few naturally occurring AAVs being described over the last five years[28–30]. However, isolation of novel AAV from more distant species may generate AAV not neutralized by human sera. Previously, we identified a porcine-derived AAV named AAVpo1, which was not neutralized by pooled human immunoglobulin G (IgG) from over 10,000 donors[30]. Pig heart valves have been used successfully in xenotransplants in human recipients supporting the hypothesis that porcine-derived AAVs would perform well and have low associated toxicity in humans[31].

In this study, we describe the *in vitro* and *in vivo* characterization of 4 novel porcine AAVs: AAVpo2.1, AAVpo4, AAVpo5, and AAVpo6, which were selected and generated from a pool of over 20 new isolates. Two additional *cap* sequences were also isolated (AAVpo7 and AAVpo8) but surprisingly failed to generate functional particles. The newly isolated porcine AAV vectors belong to three new clades within the AAV family. Several porcine-derived AAVs demonstrated preferential tropism for specific tissue in mice. These results contribute to a broader understanding of several new AAV vectors isolated from porcine tissues that were not neutralized by human sera at detectable levels.

Results

AAV genomes exist within pig genomic DNA. In order to isolate novel porcine AAV vectors, genomic DNA was isolated from pig gut and then screened for the presence of AAV sequences by using primers specific for conserved regions of the AAV genome. These primers were designed to isolate a region spanning approximately 900 base pairs (bp) of the 3′-end of the AAV *rep* gene and 800 bp of the 5′-end of the AAV *cap* gene, for a total screening product of 1.7 kilobases (kb). A pool of over 25 porcine AAV isolates was generated using this technique and named in the order that they were identified (Fig. 1a). Sequence data for AAVpo9 - AAVpo21 and AAVpo23 - AAVpo26, for which completed sequences could not be isolated, was submitted to GenBank (accession numbers KM34829 – KM34847). The complete *cap* genes for AAVpo4, -po5, -po6, -po7, and -po8 were isolated by nested thermal asymmetric interlaced (TAIL) polymerase chain reaction (PCR) and cloned into an expression vector along with AAV2 *rep*. We previously reported partial sequence of 3′-end of *cap* for AAVpo2, which shared ~80 percent sequence homology to AAV2[30]. From the newly obtained AAV sequences, AAVpo2 was found to share 95.2 percent homology with AAVpo6. We conceptualized that the high homology between the two AAVs could possibly allow for production of viable rAAV hybrid particles. The first 255 base pairs (bp) of AAVpo6 *cap* were used to complete a hybrid capsid of both AAVs, resulting in the production of viable particles called AAVpo2.1, as previously described[29]. VP1 sequence data for AAVpo2.1, -po4, -po5, and -po6, has been submitted to GenBank (accession numbers JX896665, JX896667, JX896666, and JX896664, respectively).

Successful production of porcine-derived rAAV vectors expressing β-galactosidase (LacZ) was achieved via triple transfection of helper, packaging, and transgene plasmids using a calcium phosphate transfection method. Briefly, *trans*-packaging plasmid consisting of porcine-derived AAV *cap* and AAV2 *rep*, *cis*- plasmid containing LacZ flanked by AAV2 ITRs, and the helper plasmid pAdΔF6, were transfected into HEK293T cells producing chimeric rAAV particles. To confirm viral particle production, VP1, VP2, and VP3 capsid protein expression was examined by western blot analysis for AAVpo2.1, -po4, -po5, -po6, and AAV5 as controls from transfected cellular pellet (Fig. 2). Curiously, despite the fact that full *cap* genes were isolated for AAVpo7 and –po8 (accession numbers KM349848 and KM349849, respectively), capsid proteins for these isolates by western blot could not be detected.

Porcine-derived AAVs form new clades. One major goal of this work was to isolate novel AAVs with distinct properties from existing ones, with the possibility of belonging to new clades. All phylogenetic analyses were conducted using Clustal W or multiple sequence comparison by log-expectation (MUSCLE) alignments and trees were generated using neighbor-joining method. The translated amino acid (aa) sequence for the first ~800 bp of the 5′-end of isolated porcine AAV cap were aligned with the corresponding regions of known AAVs representing each previously defined clade[27]. If three or more sequences formed a monophylic group and were within a genetic distance of 0.09 from one another, they were considered to belong to the same clade. Here, three new clades were identified named Clade G, H, and I (Fig. 1a). Once the unique AAV sequences were identified, complete *cap* genes were produced for 5 of the novel porcine AAVs representing each new clade, thereafter denoted AAVpo4, -po5, -po6, -po7, and -po8. From Fig 1a, AAVpo7 and –po8 were grouped in the same clade with a genetic distance of 0.03. However, when complete cap sequences were aligned, their genetic distance changed to 0.30, altering the phylogenetic relationship between AAVpo7 and –po8. AAVpo7 was positioned in the same grouping as AAVpo4 and –po6, but was not considered monophylic due to its genetic distance from the latter two AAVs (0.121 and 0.100, respectively).

An aa alignment was performed between AAV1, -2, -po1, -po2.1, -po4, -po5, -po6, -po7, and –po8, and translation of VP1, VP2, and VP3 products is indicated by arrows (Fig. 3). Many of the porcine-derived AAVs formed new clades within the AAV family with AAVpo2.1, -po4, and –po6 aa sequences situated more closely to AAV2 having 83.5%, 82.1%, and 83.1% similarity, respectively (Table 1). In contrast, AAVpo5 was closer to AAVpo1 and AAV5 with 92.1% and 88% aa sequence homology, respectively (Table 1).

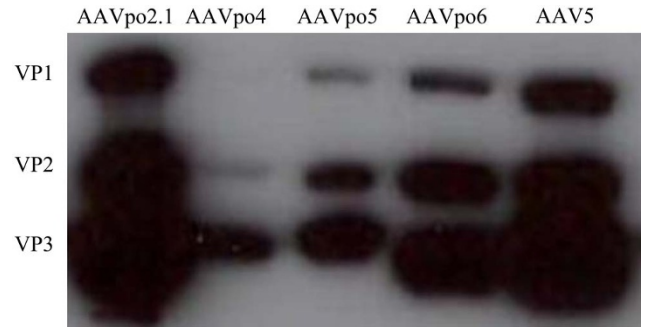

Figure 2 | Porcine-derived AAVs form VP1, VP2, and VP3. DNA encoding the *cap* of porcine-derived AAVs was transfected into HEK293T cells. Cell lysate was harvested and western blot performed using monoclonal antibody against AAV VP1, VP2, and VP3 (Fitzgerald). Western blot reveals that porcine-derived AAVs form VP1, VP2, and VP3 with sizes of ~87, 72, and 62 kiloDaltons, respectively. AAV5 VP1, VP2, and VP3 were used as a comparison.

AAVpo7 homology was found to be closer to AAV2 and AAVpo2.1 with 80.1% and 91.9% homology, respectively, whereas AAVpo8 was mostly divergent from known AAVs of primate or porcine origin, with its nearest relatives being AAV3 and AAVpo7 at 65.7% and 75.1% homology, respectively.

Porcine-derived AAVs are not neutralized by pooled human IgG. Pre-existing immunity towards current AAV vectors can be a major drawback for their use in the clinic, and consequently, low seroprevalence in the human population is desirable to obtain optimal efficacy. Neutralization assays were performed on porcine-derived AAVs using pooled human IgG from 10,000 to 60,000 donors (CLS Behring). Briefly, each LacZ expressing AAV vector was incubated with pooled human IgG or with antisera obtained from mice vaccinated with the same AAV vector, or other porcine or human AAVs at various dilutions, followed by detection of the reporter gene on target cells. Human IgG failed to neutralize the porcine-derived AAVs, with the exception of AAVpo6, where a relatively high concentration (1.5 mg/mL) of pooled human IgG neutralized 50% of vector particles. In contrast, 0.1875 mg/mL of pooled human IgG neutralized AAV5, while AAV1, -5, -6, and -8 expressing LacZ were not neutralized by any of the anti-sera produced against porcine-derived AAVs (Table 2). Mouse sera obtained from AAV-LacZ vector immunization neutralized the corresponding AAV vector that the mouse was vaccinated with, but not other AAV serotypes, showing that each porcine-derived AAV is a distinct serotype (Table 2). A possible exception was AAVpo6, which was neutralized by AAVpo2.1 antisera at a 1 : 40 dilution, in contrast to the 1 : 640 dilution of the antisera from AAVpo6 vaccinated mice required to neutralize it.

Porcine-derived AAVs elicit specific tissue tropisms in mice. To look at biodistribution and dissemination, each AAV vector expressing LacZ was delivered through intravenous tail vein (IVTV) injection at a dose of 1×10^{11} genome copies (gc) per mouse. Mice were sacrificed 28 days post-infection to allow for sufficient gene expression and tissues were harvested. Samples were considered positive for the presence of AAV vector genomes if gc values from real time (RT)-PCR were at least three times that of the negative control. AAVpo5 was shown to perform very poorly in the biodistribution studies, with levels similar to the negative control and a low mean gc/cell across the board for all the major organs tested. When delivered systemically, AAVpo2.1 performed poorly in all major organs tested, much like AAVpo1. However, AAVpo2.1 preferentially targeted kidneys and muscle, as higher titers were obtained in these particular organs relative to other sampled tissues (Fig. 4). Transduction efficiencies were similar for AAVpo4 and –po6 with above background titers detected in every organ sampled, with the highest found in the liver where an average of 61.859 and 20.980 gc/cell were measured, respectively. Most interestingly, intravenous administration resulted in the presence of AAVpo4 and –po6 gc in the mouse brain at titers of 0.188 gc/cell and 0.147 gc/cell, respectively. In contrast, 0.013 and 0.002 gc/cell were found in the brain for AAVpo2.1 and –po5, respectively. The presence of AAVpo4 and –po6 in the brain raises the possibility that these two vectors can cross the blood-brain barrier to reach the central nervous system (CNS).

Certain porcine-derived AAVs transduce the mouse lung, liver, and muscle. To assess the ability of porcine-derived AAVs to transduce lung tissues from the apical side (airway side), AAV vectors were administered to BALB/c mice by intranasal instillation and lungs were harvested 28 days post-injection and analyzed by histochemistry of the LacZ gene product on frozen sections. All but AAVpo6 of the porcine-derived AAVs performed poorly in the mouse lung. AAVpo6 transduced both airway epithelia and cells in the lung parenchyma at efficiencies comparable to AAV5, which was

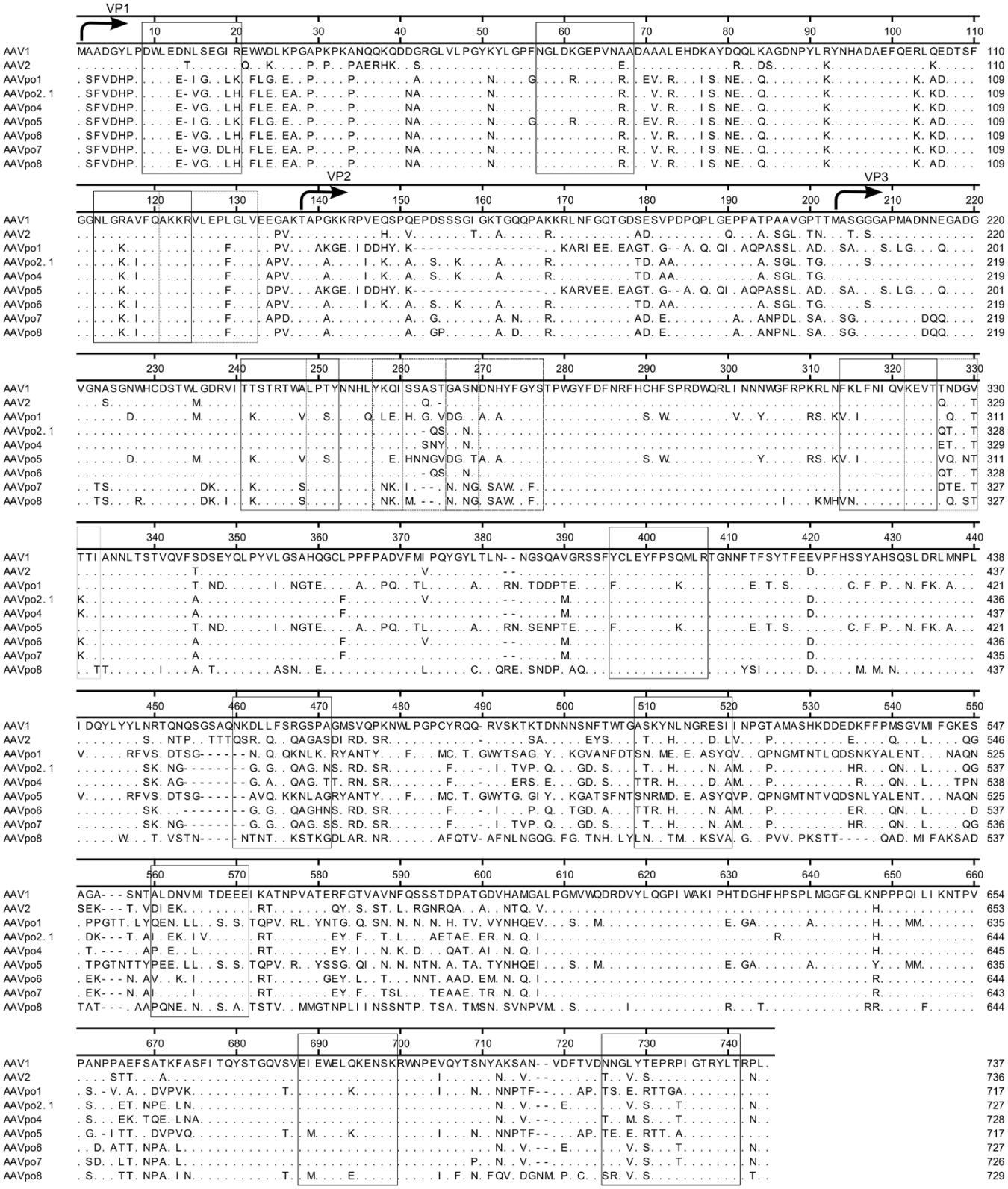

Figure 3 | Porcine-derived AAV capsid proteins are highly divergent. The amino acid sequences of porcine-derived AAV capsid protein VP1 were aligned with the amino acid sequences of AAV1 and AAV2. Arrows indicate the putative translation start sites for VP1, VP2, and VP3. The consensus sequence is based on AAV1, where amino acids listed for all other AAVs indicate a difference at that position, dots (.) indicate similar amino acids to that of AAV1, whereas dashes (-) indicate an absence of amino acids. The amino acid sequences in solid, dotted, or dashed boxes represent the common AAV2 VP1 epitopes recognized by human PBMCs (Madsen *et al.*, 2009).

Table 1 | Percent homology of porcine-derived AAV capsid sequences with published AAV sequences

	Amino Acid Identity (%)					
	AAVpo2.1	AAVpo4	AAVpo5	AAVpo6	AAVpo7	AAVpo8
AAVpo2.1	-					
AAVpo4	93.5	-				
AAVpo5	62.1	63.5	-			
AAVpo6	95.2	92.3	62.6	-		
AAVpo7	91.9	88.3	61.4	90.2	-	
AAVpo8	70.5	70.6	59.8	70.7	75.1	-
AAV1	79.4	80.1	58.1	79.6	77.4	64.3
AAV2	83.5	82.1	59.2	83.1	80.1	65.1
AAV3	80.7	80.6	59.6	81.1	78.9	65.7
AAV4	59.8	59.4	54.2	59.8	58.7	56.7
AAV5	61.1	61.8	88	61.6	60.5	59.5
AAV6	79.2	79.8	57.7	79	77.1	64.3
AAV7	79.9	80.2	59.3	79.5	77.4	65.3
AAV8	80.5	79.9	59.9	80.6	78	65
AAV9	80.6	80.5	58.8	80.2	78.4	64
AAVrh.32.33	60.3	60.4	55.2	61.2	59.8	58.8
AAVpo1	62.4	63.5	92.1	62	61.4	59.5

previously described as a good transducer of airway epithelial cells relative to other primate AAVs (Fig. 5; 34, 35).

In order to evaluate the performance of porcine-derived AAVs in liver tissue, each AAV vector was delivered systemically through intravenous injection of the lateral tail vein and the liver was harvested 28 days post-injection. Liver sections from IVTV injected mice were embedded in O.C.T. medium, and histochemistry and 5-bromo-4-chloro-3-indolyl-β-D-galactopyranoside (X-gal) staining was performed to visualize β-gal activity of transduced cells (Fig. 6). AAV8, a 'gold-standard' vector for transduction of hepatocytes, was administered at 1×10^{11} gc/mouse via IVTV and used as a comparison to evaluate the performance of the porcine-derived AAVs. Consistent with previous studies, AAV8 administration resulted in high gc numbers detected in the liver[34]. Interestingly, we found that the average number of gc/cell present in the liver for AAV8 injected mice (52.414) was very similar to that of animals injected with the AAVpo4 vector (61.859), $p > 0.05$. Transduction of hepatocytes following injection of AAVpo4 and –po6 mainly substantiated the RT-PCR biodistribution data with gc of 61.859 and 20.980, respectively. We found only anecdotal or no evidence of hepatic transduction from mice injected with AAVpo1, AAVpo2.1 or AAVpo5.

AAVs have been extensively shown to be strong gene transfer vehicles in muscle fibers following direct injections[12]. Each porcine-derived AAV vector was administered into the tibialis anterior muscle of BALB/c mice at a titer of 1×10^{11} gc, and the muscle were harvested at days 7, 14, 21, and 28 post-injection, with histochemistry and X-gal staining performed to reveal transduction efficiency at each time point. For levels of X-gal expression from the various porcine-derived AAVs, the rankings from highest to lowest are as follows: AAVpo6 > AAVpo4 > AAVpo5 > AAVpo2.1 (Fig. 7a). AAV1, one of the most efficient AAVs for transduction of muscle fibres, was injected alongside the porcine-derived AAVs as a comparison, and β-gal expression was quantified using a β-gal Assay kit (Genlantis). Peak expression levels of β-gal were achieved by AAVpo6 by day 14, while expression from the AAVpo4 vector did not reach similar levels until day 28 (Fig. 7b). β-gal expression was not measurable for AAVpo2.1 using our methods up until day 14, although minimal expression was observed on stained sections by day 7 (Fig. 7b). AAVpo5 appeared to have consistent β-gal expression throughout all time-points, albeit peak levels were relatively low compared to more efficient AAV vectors (AAVpo4, -po6, and AAV1; $p < 0.001$). AAVpo6 was the most efficient porcine-derived AAV at transducing the muscle, and had expression levels similar to that of AAV1 ($p > 0.05$).

AAVpo4 and –po6 can bypass the blood-brain barrier when delivered systemically and transduce cells in the mouse brain. From the biodistribution studies, of interest to note was the presence of rAAV genomes in the brain following AAVpo4-LacZ and –po6-LacZ IVTV injection, suggesting that these vectors may be able to traverse the blood-brain barrier and transduce cells in the

Table 2 | Neutralization antibody assay of porcine-derived AAVs and published AAVs against homologous or heterologous antisera and pooled human IgG

	Vector							
*Anti-sera	AAVpo2.1	AAVpo4	AAVpo5	AAVpo6	AAV5	AAV1	AAV6	AAV8
AAVpo1	<1:20	<1:20	<1:20	<1:20	<1:20	<1:20	<1:20	<1:20
AAVpo2.1	1:320	<1:20	<1:20	1:40	<1:20	<1:20	<1:20	<1:20
AAVpo4	<1:20	1:640	<1:20	<1:20	<1:20	<1:20	<1:20	<1:20
AAVpo5	<1:20	<1:20	1:40	<1:20	<1:20	<1:20	<1:20	<1:20
AAVpo6	<1:20	<1:20	<1:20	1:640	<1:20	<1:20	<1:20	<1:20
AAV5	<1:20	<1:20	<1:20	<1:20	1:5120	n/a	n/a	n/a
**Pooled Human IgG (mg/mL)	>12	>12	>12	1.5	0.1875	n/a	n/a	n/a

*Values represent dilution of anti-sera required to neutralize >50% of AAV-LacZ transducing particles.
**Values represent concentration of antibody in mg/mL, required to neutralize >50% of AAV-LacZ transducing particles.

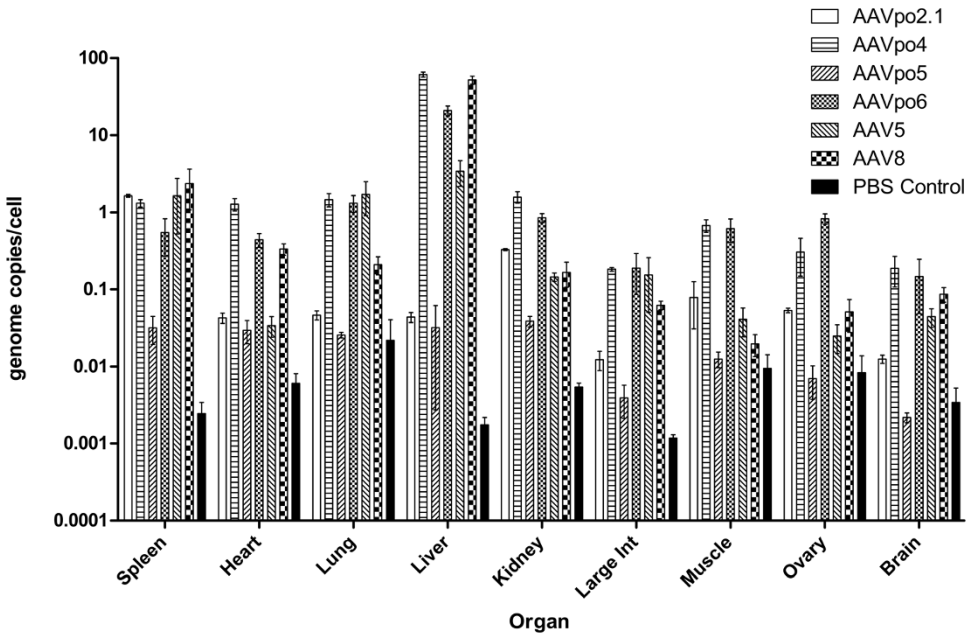

Figure 4 | Porcine-derived AAVs are present in a multitude of mouse tissues when delivered systemically. Porcine-derived AAVs expressing LacZ were administered intravenously in the lateral tail vein of BALB/c mice and organs harvested 28 d.p.i. DNA was extracted from the organs and RT-PCR performed to reveal the average gc/cell present per organ. AAV5 and AAV8 were used as positive controls, whereas PBS injected mice were used as negative controls. Much like AAV8, AAVpo4 and –po6 were present in most major organs when delivered systemically. AAVpo2.1 seemed tropic for spleen, kidney, and muscle, whereas AAVpo5 had levels comparable to the negative control in virtually all organs sampled. Surprisingly, the presence of AAVpo4 and –po6 were also detected in the mouse brain. $n = 3$ mice, data presented as the mean ± SEM.

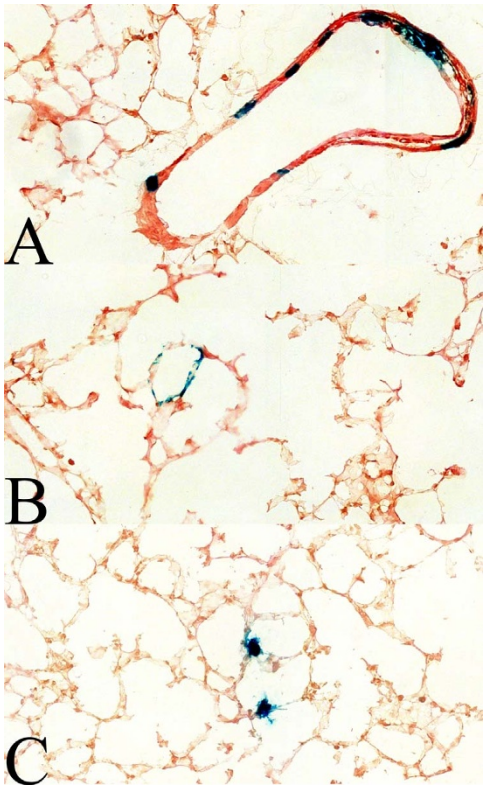

Figure 5 | AAVpo6-LacZ transduce cells in the mouse lung parenchyma and airway epithelia. AAVpo6-LacZ was instilled intranasally into mice at 1×10^{11} gc/mouse. Lungs were harvested 28 d.p.i., frozen with O.C.T., and cryosectioned at 10 μm. Each section was stained with X-gal and eosin. Blue colored cells are indicative of transduced cells. (a) Airway epithelia, and (b, c) lung parenchyma.

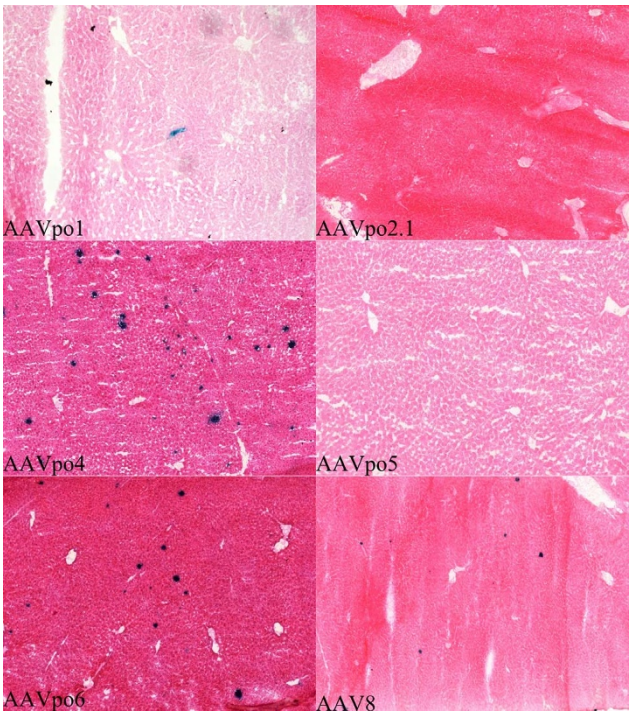

Figure 6 | Porcine-derived AAVs transduce cells in the mouse liver. Porcine-derived AAVs expressing LacZ were delivered IVTV into mice at a titer of 1×10^{11} gc/mouse, and liver was harvested 28 d.p.i. Livers were frozen with O.C.T., cut into 10 μm sections, and stained with X-gal and eosin. Blue cells are indicative of AAV-LacZ transduced cells. AAV8 was used as a control.

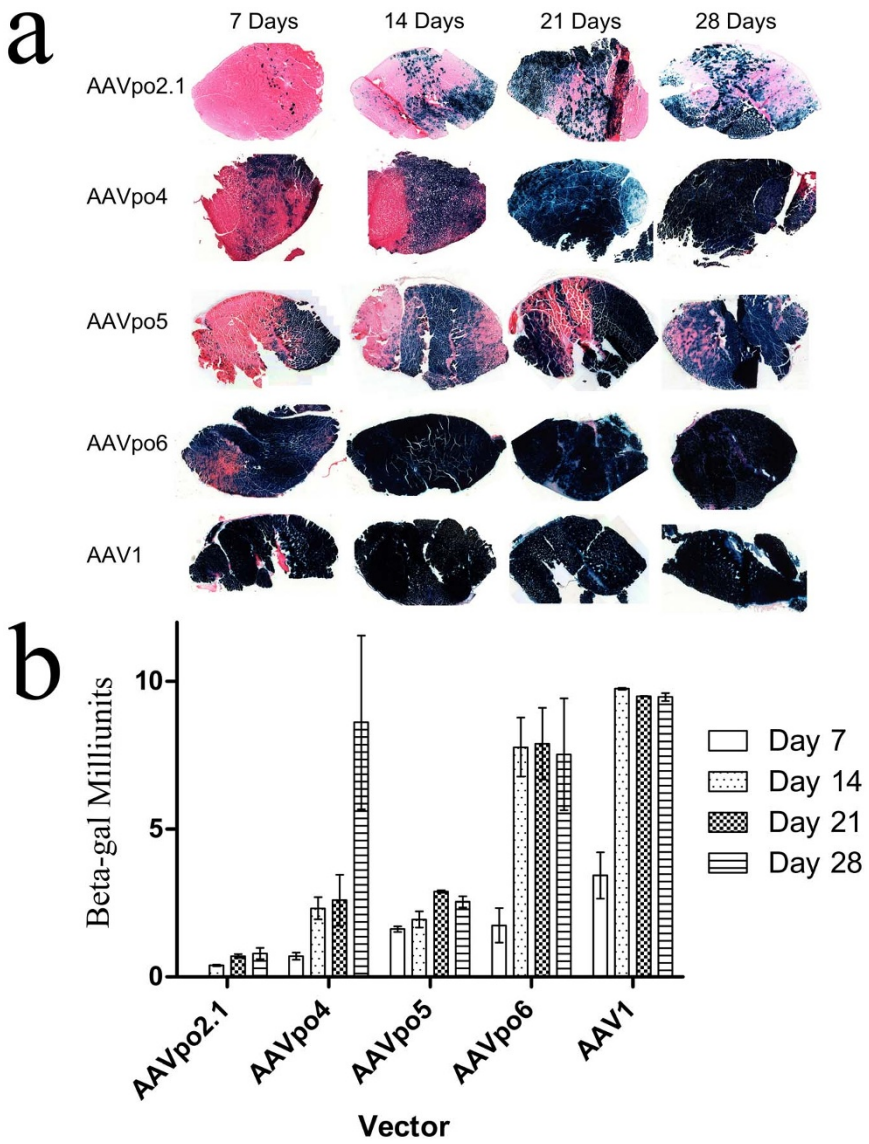

Figure 7 | Porcine-derived AAVs transduce cells in the mouse muscle. Porcine-derived AAV-LacZ vectors were administered IM at a dose of 1×10^{11} gc/mouse and muscle harvested at various time-points. (a) Muscle was harvested at Days 7, 14, 21, and 28 post-injection. Muscle was frozen with O.C.T. and cryosectioned in 10 μm sections, and stained with X-gal and eosin. Blue cells are indicative of AAV-LacZ transduction. AAV1 was used as a control. (b) AAV-LacZ transduced muscle was harvested at 7, 14, 21, and 28 days post-injection and subjected to a β-gal expression assay. Values represent the mean ± SEM. $n = 3$ mice.

CNS. To evaluate direct versus peripheral administration of vector, 6–8 week old BALB/c mice were injected either intracranially (IC) or by IVTV with the AAV-LacZ vectors. Brains were harvested 28 days post-injection, and histochemistry and X-gal staining was performed on cut sections. For brain samples from IVTV injected mice, transduction by AAVpo4 and -po6 can be observed in different areas of the brain including (Fig. 8), although AAVpo4 was not nearly as efficient as AAVpo6. In these conditions, transduced cells from AAVpo4 and -po6-LacZ vectors were detected in the olfactory bulb, striatum, hippocampus, cortex, hypothalamus, and medulla areas of the CNS. However, only AAVpo6 was observed in the cerebellum following intravenous administration. Following IC administration, AAVpo6 transduced cells were mainly localized at the site of injection, albeit at a relative good level with migration of the positive staining away from the delivery site reaching the forebrain (striatum, hippocampus), midbrain, and hindbrain (cerebellum) areas of the CNS, whereas AAVpo4 remained localized and transduced cells in the hippocampus and striatum. These results support the concept that AAVpo4 and -po6 could traverse the intact blood-brain barrier, consistent with the results obtained from the biodistribution studies.

Discussion

The focus on developing new AAV vectors has been placed primarily on designer AAVs through methods such as directed evolution, decoration of capsid particles with random peptide display, PEGylation, or genetic alteration of B cell epitopes on the capsid surface to prevent recognition by pre-existing neutralizing antibodies[20,22,35–38]. Although these methods have produced particles shielded from pre-existing humoral immunity, the effect is mostly incomplete and there still remains the problem of T cell epitopes and activation of cell-mediated immunity, which can abrogate gene expression in transduced tissue. T cell epitopes are not limited to the external surface of the capsid and can be found internally as well[39–41]. An example adverse host T cell responses against the AAV capsid was seen in a clinical trial involving AAV2-FIX in human liver, in which

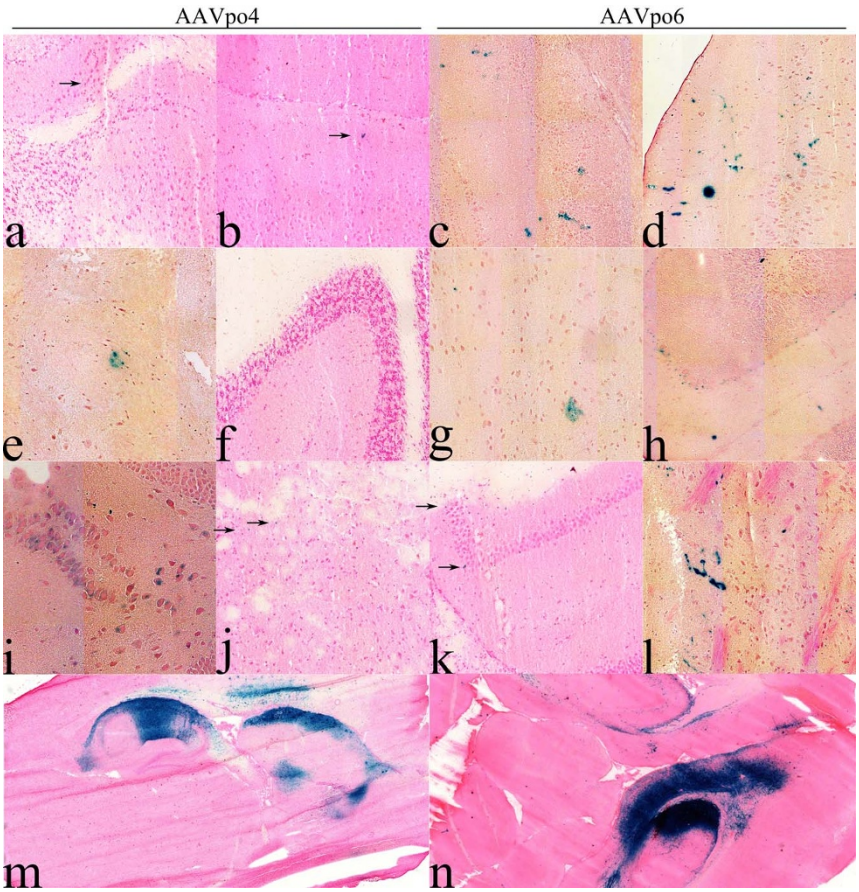

Figure 8 | Porcine-derived AAVs transduce cells in the mouse brain. AAVpo4-LacZ and –po6-LacZ were assessed for their ability to transduce cells in the CNS of BALB/c mice following IVTV or IC administration of AAVpo4-LacZ or –po6-LacZ at a titer of 1×10^{11} gc/mouse. Following IVTV injections, AAV-LacZ transduction was observed in: (a, c) olfactory bulb, (e,g) striatum, (i, k) hippocampus, (b,d) cortex, (f, h) cerebellum, and (j, l) medulla of the mouse brain. (m, n) Cross sections of mouse brains injected IC with AAV-LacZ vectors. Mouse brains were frozen with O.C.T. and sectioned using a cryostat at 10 μm. Each section was stained with X-gal and eosin or nuclear fast red stain. Blue cells represent AAV-LacZ transduced cells (anecdotal transduction is indicated by black arrows).

FIX levels were detected early after administration of vector, yet levels dropped significantly within 4–6 weeks in several subjects[42]. Another study showed $CD8^+$ T cell generated against AAV2 capsid epitopes are cross-reactive with AAV8 capsid[43]. Genetically similar serotypes may share the same T cell epitopes, explaining why gene expression was abolished, as seen in several clinical trials[42,44,45]. This places substantial limitation to the uses of existing human and non-human primate AAVs if they indeed share similar T cell epitopes. Since neutralizing antibodies towards AAV2 can be found in up to 90% of the human population, there remains the risk that genetically similar AAVs may cross-react with T cells generated against AAV2. Here, porcine-derived AAVs shared some of the common AAV2 epitopes recognized by human PBMCs, yet other epitopes also displayed subtle differences[41]. More experimentation will need to be performed to determine if indeed, porcine-derived AAV epitopes are cross-reactive with AAV2 specific T cells.

Isolation of divergent AAVs is important, as they may be able to circumvent T cell cross-reactivity. In our study, we were able to isolate several new AAVs from porcine tissues, which belong to new clades and are genetically diverse from other previously described primate and porcine-derived AAVs; an exception was AAVpo5, which was genetically similar to AAVpo1. That pooled human IgG failed to neutralize porcine-derived AAVs, (except for AAVpo6, which required a relatively higher concentration to be neutralized) bodes well for their use in humans.

The majority of the porcine AAVs (AAVpo4, AAVpo5, and AAVpo6) were isolated from the gut of a single pig out of 8 pigs, suggesting that this animal was undergoing an active, natural AAV infection. From this pig, we observed more than 20 novel AAV isolates belonging to 3 divergent and unique clades. Gao *et al* observed diversity in a multitude of AAV sequences isolated from monkey tissues, and attributed this to homologous recombination of different parental AAV serotypes, with mutation rates at levels similar to RNA viruses[46]. Recombination during active AAV infection may explain how we identified a large number of AAV isolates, as well as the identification of the non-functional AAVpo7 and –po8 isolates. Nevertheless, we were able to identify several functional AAVs displaying unique tissue tropisms and transduction efficiencies from one another. Selective pressure during active AAV infection may allow for optimization of virus particles, providing a rationale supporting natural hosts to be considered and not overlooked for sources of novel AAVs. As well, the identification of AAVs belonging to new clades may add to the genetic diversity of existing AAV vectors, as well as improve upon vector targeting and transduction efficiency. Biopanning of AAVs, which arose from directed evolution, was performed in mice to select for AAVs with shuffled *cap* genes and tropic for specific organs including the lung and liver[47]. It would be of interest to perform the same technique in pigs, a species considered close to humans.

Previously, AAVpo1 was shown to preferentially target muscle fibres[30]. Similarly, AAVpo2.1 demonstrated a preferential tropism for the heart, kidney, and muscle, and like AAVpo1, may be useful for systemic delivery. An intriguing characteristic of AAVpo2.1 is that it is not genetically similar and belongs to a new clade separate

from AAVpo1. Another peculiar AAV was AAVpo5, which performed very poorly in biodistribution studies. Although AAVpo5 genomes appeared to be absent in the tibialis anterior muscle of intravenously injected mice, consistent levels of β-gal expression throughout different time-points were detected in intramuscularly (IM) injected mice starting from day 7. Since AAVpo5 genomes were absent or low in the biodistribution studies, perhaps AAVpo5 cannot pass through blood vessels as easily, conceivably making it a safe vector to inject into specific organs without leakage into the bloodstream. This would be beneficial for treatment in specific organs such as the muscle or eye. The efficacy of AAVpo5 in murine and porcine retina was evaluated and shown to efficiently transduce cell types such as the retina and photoreceptors[29].

Apart from vectors with preferential organ tropism, two porcine-derived AAVs demonstrated robust transduction in a multitude of tissues. AAVpo4 and –po6 genomes were present in nearly every organ sampled when injected intravenously. Although we did not investigate receptor specificity of porcine-derived AAVs, perhaps the tissues that are transduced share similar receptors/co-receptors, or these AAVs may be able to bind to more than one type of receptor. Although AAVpo4 and –po6 were not tested in parallel with AAV9, they appear to have similar transduction efficiency profiles[48]. AAV9 was shown to pass through the blood-brain barrier and transduce cells in the brain when delivered systemically, similar to AAVpo6[14]. To complement this, AAVpo6 also showed efficient transduction in airway cells following intranasal injection, much like AAV9[49]. These observations could be explained by the use of a common receptor that was described for AAV9, N-linked galactose. Follow up studies will need to be performed to evaluate the cellular receptors of AAVpo4 and –po6.

Previous transduction of AAV9 in the mouse brain through IVTV administration was performed using titers up to 4×10^{12} gc/mouse, and self-complementary AAV genomes expressing GFP in neonates and adult mice, with transduction limited to astrocytes and neuronal cell in adult mice[14]. In the present study, single-stranded recombinant AAV genomes at a titer of 1×10^{11} gc in adult mice demonstrated transduction in several areas of the CNS.

Apart from transduction efficiency in the brain and lung, AAVpo6 also showed high efficiency in the mouse muscle. As a comparison, we utilized AAV1, one of the most efficient AAVs for transducing muscle fibers, and found that AAVpo6 produced levels similar to this vector. Therefore, consideration should be placed upon AAVpo6 as a vector for treatments in the lung, brain, and muscle.

Although AAVpo4 and –po6 had similar biodistribution profiles in most organs, AAVpo4 produced 3-fold more gc in the liver compared to AAVpo6. To compare the efficiency of AAVpo4 in the liver, we injected mice via IVTV with AAV8, which is considered one of the most efficient AAVs for transduction of hepatic tissues. We found that both AAV8 and AAVpo4 transduced the liver at similar levels. AAVpo4 can be considered an alternative to AAV2 and AAV8 and future treatments exploiting its efficiency in the liver may be useful for treatment of genetic ailments such as human Factor IX deficiency or α1-antitrypsin deficiency. Although porcine-derived AAV transduction efficiency in mouse does not necessarily represent transduction efficiency in human tissue, more studies will need to be performed in higher animal models closer to humans. From our findings, AAVs isolated from pigs should be considered for future gene therapy applications due to the lack of pre-existing immunity against porcine-derived AAVs, as well as their unique tissue tropism profiles.

Methods

Identification and Phylogenetic Analysis of AAV Genomic DNA. AAV genomic DNA for AAVpo2.1, -po4, -po5, –po6, -po7, and –po8 were isolated from pig genomic DNA as previously described[29]. Genomic DNA was isolated from pig guts using a QIAamp DNA mini kit (Qiagen). PCR was carried out on pig genomic DNA and screened for the presence of AAV using primers RC^{+}: 5′-GGTGCGTAAACTGGACCAATGAGAAC-3′ and SIG^{-}: 5′-GAATCCCCAGTTGTTGTTGATGAGTC-3′, to isolate a 1.7 kb fragment spanning ~900 bp for the end of *rep* and ~800 bp for the beginning of *cap* as previously described[30]. The signature region of the *cap* gene (variable between all AAVs) was contained within this fragment as described elsewhere[50]. Basic Local Alignment Search Tool (BLAST) analysis was performed to determine if the sequences were unique. The beginning of isolated AAV *cap* genes consisting of ~800 bp was translated and aligned with similar regions of other published AAVs using Clustal W method of MegAlign (DNAstar Lasergene 9.0) or MUSCLE method of MEGA6. Pairwise distance between sequences was calculated and analyses conducted using the Poisson correction model. The evolutionary history was inferred using the Neighbor-Joining method. Phylogenetic trees were drawn to scale, with branch lengths in the same units as those of the evolutionary distances used to infer the tree. Clades were identified as previously defined[27]. Briefly, three or more monophylic sequences within a genetic distance of 0.09 from one another were considered a clade. Several isolates representing each clade were selected and nested TAIL-PCR was performed to isolate full AAV *cap* genes, using the primers $Nestedcap1^{+}$2.7 kb (5′-TGGAGGACCGAATGTTCAAGTTTG-3′), $Nestedcap2^{+}$2.4 kb (5′-CGACCGATCGATTGGACCTC-3′), and $Nestedcap3^{+}$2.2 kb (5′-AAGCGAGTAGTCATGTCGTTG-3′)[29]. The degenerate primer utilized was CED^{-} (5′-ACTGAMACGAAT(H/-)AMMCGGTTTATTGA-3′), as previously described[29]. Although partial pig AAV DNA (~800 bp) of the 5′ end of the *cap* was confirmed from the PCR screening matching 100% to the same regions from the completed pig AAV *cap* sequences, and sequences isolated from the primary nested TAIL reaction matched 100% to the sequences in the secondary reaction for those sequences that were available (data not shown), completed *cap* sequences were not verified from the source. Therefore, there exists the possibility that artefacts may have arisen nearer to the 3′ end of the pig AAV *cap* sequences due to the use of a degenerate primer. The amino acid sequences of full AAV *cap* isolated from porcine tissues were aligned with AAV1, AAV2, and our previously identified AAVpo1 (accession numbers AF063497, NC_0011401, and FJ688147, respectively). The aligned sequences were evaluated for the presence of AAV2 VP1 epitopes recognized by human peripheral blood mononuclear cells[41].

Recombinant AAV vector production. Once isolated, the AAV *cap* gene was cloned into a *cis* plasmid expression vector encoding AAV2 *rep*. Triple transfection was performed with CalPhos Mammalian Transfection Kits (Clontech Laboratories) using the *cis* plasmid (encoding AAV2 *rep* and AAV *cap*), *trans* plasmid (encoding LacZ transgene flanked by AAV2 ITRs), and pAdΔF6 helper plasmid (containing Adenoviral genes to drive generation of recombinant AAV particles) in HEK293T cells. Cells were incubated at 37°C with 5% CO_2, then harvested 72 hours post-transfection and spun for clarification. Supernatant from the clarification step was collected, then overlayed onto cesium chloride (CsCl) gradients for purification. The particles were then spun thru Amicon Ultracel -100K filters (Millipore) and concentrated into ~1.8 mL. Cells were grown with Delbecco's modified Eagle's medium (DMEM) supplemented with 10% fetal bovine serum (FBS) and 1% penicillin/streptomycin. AAV1-LacZ was kindly provided by the Vector Core at the University of Pennsylvania.

AAV Capsid Protein Characterization. Porcine AAV VP1 proteins were characterized using Protean of the DNAStar Lasergene 9.0 software package to reveal predicted aa lengths and weights. Porcine-derived AAV capsid DNA was transfected into HEK293T cells, then harvested using 1X radio immunoprecipitation assay (RIPA) buffer. Samples were mixed with loading buffer and boiled at 90°C for 10 minutes. Samples were then loaded onto polyacrylamide gel and supplied with 200 V for 1 hour. Monoclonal antibodies for AAV capsid proteins VP1 + VP2 + VP3 (Fitzgerald) were used in western blot analysis to visualize the AAV capsid proteins.

Neutralizing Antibody Assay. AAV capsid were injected IM into the tibialis anterior of mice at a dose of 1×10^{11} gc/mouse, and blood was collected via cardiac puncture 28 days post-injection. Serum was separated and collected using serum separator tubes (BD). Serum was then heated to 56°C for 45 minutes to inactivate complement. Porcine-derived AAV-LacZ particles were incubated with heat inactivated sera for 1 hour, then transferred onto HEK293T cells (giving ~100 transduced cells per well) in a 96-well format for an additional hour. Supplemented media was added following incubation. 48 hours post-infection, cells were fixed using 1.6% glutaraldehyde in phosphate buffered saline (PBS), and incubated with X-gal staining solution at 37°C with 5% CO_2 overnight. Neutralization titer was reported as the reciprocal of the highest dilution for serum able to neutralize ~50% of transducing particles compared to PBS incubated particles. In a similar fashion, pooled human IgG (CSL Behring) were incubated with AAV-LacZ particles, starting at a concentration of 12 mg/mL, with a 2-fold dilution going down each well. Neutralization was reported as the reciprocal of the highest dilution where ~50% of transducing particles were neutralized when compared to the non-neutralized control wells.

Biodistribution Studies in Mice. Mice were injected with AAV-LacZ via IVTV route at a vector dose of 1×10^{11} gc/mouse in 100 μL (diluted with PBS), using a 27 gauge, ½ inch needle (BD). 28 days post-injection, the following organs were harvested: spleen, pancreas, heart, lung, liver, kidney, small intestine, large intestine, ovaries, tibialis anterior muscle, and brain. ~25 mg of tissue from each organ was collected and lysed using a Qiagen TissueLyser. DNA was extracted using QIAamp DNA Mini kits (Qiagen) as per manufacturer instructions. Quantitative real-time PCR (RT-PCR) was performed on genomic DNA using a LightCycler 480 (Roche) and the

primers BGHFW (5′-TCTAGTTGCCAGCCATCTGTTGT-3′) and BGHREV (5′-TGGGAGTGGCACCTTCCA-3′), and probe (6FAM-TCCCCCGTGCCTTCCTTGACC-TAMRA). Signals 3 times that of the PBS control were considered positive for recombinant AAV genomes. Results were reported as the average number of gc present per cell.

Histology and β-gal expression. All mice used for histology purposes were injected with AAV-LacZ at a vector dose of 1×10^{11} gc/mouse. For mice injected intransally (IN), 50 μL of AAV-LacZ vector genomes were delivered using a P200 pipette in mice anesthetized with isoflurane. 28 days later, lung was harvested and inflated with a 1 : 1 mixture of PBS and Optimal Cutting Temperature medium (O.C.T.), then frozen in O.C.T. in a dry ice/ethanol bath. For IM injected mice, tibialis anterior muscle was injected with 50 μL of AAV-LacZ vector, and muscle was harvested at days 7, 14, 21, and 28 post-injection. 2-Methylbutane pre-chilled with liquid nitrogen was used to snap-freeze muscle tissue. Frozen muscles were then embedded using O.C.T. and placed in a cryomold on a dry ice/ethanol bath. For IVTV injections, 100 μL of vector was injected into mice. The liver and brain were harvested 28 days post injection and frozen using O.C.T., cryomolds, and a dry ice/ethanol bath. For mice injected IC in the frontal cortex, 1×10^{11} gc of vector was administered in a 10 μl volume using a Dymax Stepper™.

All tissues frozen with O.C.T. were cut using a Leica CM1850 cryostat at a thickness of 10 μM and temperature of −20°C. Cut sections were placed on Superfrost glass slides (Fisher Scientific), fixed with a 1.6% glutaraldehyde solution in PBS for 10 minutes, washed with PBS, and stained overnight with X-gal staining solution. The following day, the tissues were stained with eosin and dehydrated using 70%, 90%, and 100% ethanol baths. Alcohol was cleared using xylene, and cover slips were mounted using Permount (Fisher Scientific). Slides were scanned using a MIRAX MIDI scanner (Zeiss), and pictures were recorded using 3D Histech Pannoramic Viewer.

For β-gal assays, 10–10 μm muscle sections from various locations of the muscle were collected for each different time-point. Sections were washed with PBS to remove O.C.T. and spun down in a 2 mL cryotube. Genlantis β-gal assay kit was then used as per manufacturer instructions to determine the amount of transgene expression per sample, and presented as β-gal milliunits based on the standard curve for known amounts of β-gal. Absorbance was recorded at 570 nm.

Animal studies. Sixty-three BALB/c mice, 6 to 8 weeks old (The Jackson Laboratory, Bar Harbor, ME) were handled in accordance with the approved guidelines set by the Canadian Council on Animal Care at the National Microbiology Laboratory of the Public Health Agency of Canada.

Statistical analysis. Graph Pad Prizm software was used for statistical analysis. Data were subjected to two-way analysis of variance (ANOVA) followed by Bonferroni posttests, where appropriate. Samples were considered significantly different if $p < 0.05$. Data is presented as the mean ± standard error of the mean (SEM).

1. Hickman, M. A. *et al.* Gene expression following direct injection of DNA into liver. *Hum. Gene Ther.* **5**, 1477–83 (1994).
2. Aravindaram, K. & Yang, N. S. Gene gun delivery systems for cancer vaccine approaches. *Methods Mol. Biol.* **542**, 167–78 (2009).
3. Tsong, T. Y. Electroporation of cell membranes. *Biophys. J.* **60**, 297–306 (1991).
4. Pan, H. *et al.* Sonoporation of cells for drug and gene delivery. *Conf. Proc. IEEE Eng. Med. Biol. Soc.* **5**, 3531–4 (2004).
5. Warnock, J. N., Daigre, C. & Al-Rubeai, M. Introduction to viral vectors. *Methods Mol. Biol.* **737**, 1–25 (2011).
6. Stein, L., Roy, K., Lei, L. & Kaushal, S. Clinical gene therapy for the treatment of RPE65-associated Leber congenital amaurosis. *Expert Opin. Biol. Ther.* **11**, 429–39 (2011).
7. Mandel, R. J. CERE-110, an adeno-associated virus-based gene delivery vector expressing human nerve growth factor for the treatment of Alzheimer's disease. *Curr. Opin. Mol. Ther.* **12**, 240–7 (2010).
8. Nathwani, A. C. *et al.* Adenovirus-associated virus vector-mediated gene transfer in hemophilia B. *N. Engl. J. Med.* **365**, 2357–65 (2011).
9. Jooss, K. & Chirmule, N. Immunity to adenovirus and adeno-associated viral vectors: implications for gene therapy. *Gene Ther.* **10**, 955–63 (2003).
10. Martino, A. T. *et al.* Tolerance induction to cytoplasmic beta-galactosidase by hepatic AAV gene transfer: implications for antigen presentation and immunotoxicity. *PLoS One* **4**, e6376 (2009).
11. Jiang, H. *et al.* Evidence of multiyear factor IX expression by AAV-mediated gene transfer to skeletal muscle in an individual with severe hemophilia B. *Mol. Ther.* **14**, 452–5 (2006).
12. Louboutin, J.-P., Wang, L. & Wilson, J. M. Gene transfer into skeletal muscle using novel AAV serotypes. *J. Gene Med.* **7**, 442–51 (2005).
13. Nakai, H. *et al.* Unrestricted Hepatocyte Transduction with Adeno-Associated Virus Serotype 8 Vectors in Mice. **79**, 214–224 (2005).
14. Foust, K. D. *et al.* Intravascular AAV9 preferentially targets neonatal neurons and adult astrocytes. *Nat. Biotechnol.* **27**, 59–65 (2009).
15. Calcedo, R. *et al.* Adeno-associated virus antibody profiles in newborns, children, and adolescents. *Clin. Vaccine Immunol.* **18**, 1586–8 (2011).
16. Boutin, S. *et al.* Prevalence of serum IgG and neutralizing factors against adeno-associated virus (AAV) types 1, 2, 5, 6, 8, and 9 in the healthy population: implications for gene therapy using AAV vectors. *Hum. Gene Ther.* **21**, 704–12 (2010).
17. Hirsch, M. L., Storici, F., Li, C., Choi, V. W. & Samulski, R. J. AAV recombineering with single strand oligonucleotides. *PLoS One* **4**, e7705 (2009).
18. Zhang, Y. & Duan, D. Novel mini-dystrophin gene dual adeno-associated virus vectors restore neuronal nitric oxide synthase expression at the sarcolemma. *Hum. Gene Ther.* **23**, 98–103 (2012).
19. Halbert, C. L. *et al.* Prevalence of neutralizing antibodies against adeno-associated virus (AAV) types 2, 5, and 6 in cystic fibrosis and normal populations: Implications for gene therapy using AAV vectors. *Hum. Gene Ther.* **17**, 440–7 (2006).
20. Lee, G. K., Maheshri, N., Kaspar, B. & Schaffer, D. V. PEG conjugation moderately protects adeno-associated viral vectors against antibody neutralization. *Biotechnol. Bioeng.* **92**, 24–34 (2005).
21. Wu, Z. *et al.* Single amino acid changes can influence titer, heparin binding, and tissue tropism in different adeno-associated virus serotypes. *J. Virol.* **80**, 11393–7 (2006).
22. Müller, O. J. *et al.* Random peptide libraries displayed on adeno-associated virus to select for targeted gene therapy vectors. *Nat. Biotechnol.* **21**, 1040–6 (2003).
23. Dalkara, D. *et al.* In vivo-directed evolution of a new adeno-associated virus for therapeutic outer retinal gene delivery from the vitreous. *Sci. Transl. Med.* **5**, 189ra76 (2013).
24. Bartel, M. A., Weinstein, J. R. & Schaffer, D. V. Directed evolution of novel adeno-associated viruses for therapeutic gene delivery. *Gene Ther.* **19**, 694–700 (2012).
25. Qi, Y. F. *et al.* Comparison of the transduction efficiency of tyrosine-mutant adeno-associated virus serotype vectors in kidney. *Clin. Exp. Pharmacol. Physiol.* **40**, 53–5 (2013).
26. Mowat, F. M. *et al.* Tyrosine capsid-mutant AAV vectors for gene delivery to the canine retina from a subretinal or intravitreal approach. *Gene Ther.* **21**, 96–105 (2014).
27. Gao, G. *et al.* Clades of Adeno-associated viruses are widely disseminated in human tissues. *J. Virol.* **78**, 6381–8 (2004).
28. Li, Y. *et al.* Prevalence and genetic diversity of adeno-associated viruses in bats from China. *J. Gen. Virol.* **91**, 2601–9 (2010).
29. Puppo, A. *et al.* Recombinant vectors based on porcine adeno-associated viral serotypes transduce the murine and pig retina. *PLoS One* **8**, e59025 (2013).
30. Bello, A. *et al.* Isolation and evaluation of novel adeno-associated virus sequences from porcine tissues. *Gene Ther.* **16**, 1320–8 (2009).
31. Herring, C., Cunningham, D. A., Whittam, A. J., Fernández-Suárez, X. M. & Langford, G. A. Monitoring xenotransplant recipients for infection by PERV. *Clin. Biochem.* **34**, 23–7 (2001).
32. Zabner, J. *et al.* Adeno-associated virus type 5 (AAV5) but not AAV2 binds to the apical surfaces of airway epithelia and facilitates gene transfer. *J. Virol.* **74**, 3852–8 (2000).
33. Auricchio, A. *et al.* Noninvasive gene transfer to the lung for systemic delivery of therapeutic proteins. *J. Clin. Invest.* **110**, 499–504 (2002).
34. Inagaki, K. *et al.* Robust systemic transduction with AAV9 vectors in mice: efficient global cardiac gene transfer superior to that of AAV8. *Mol. Ther.* **14**, 45–53 (2006).
35. Huttner, N. A. *et al* Genetic modifications of the adeno-associated virus type 2 capsid reduce the affinity and the neutralizing effects of human serum antibodies. *Gene Ther.* **10**, 2139–47 (2003).
36. Yang, L., Li, J. & Xiao, X. Directed evolution of adeno-associated virus (AAV) as vector for muscle gene therapy. *Methods Mol. Biol.* **709**, 127–39 (2011).
37. Varadi, K. *et al.* Novel random peptide libraries displayed on AAV serotype 9 for selection of endothelial cell-directed gene transfer vectors. *Gene Ther.* **19**, 800–9 (2012).
38. Le, H. T., Yu, Q.-C., Wilson, J. M. & Croyle, M. A. Utility of PEGylated recombinant adeno-associated viruses for gene transfer. *J. Control. Release* **108**, 161–77 (2005).
39. Sabatino, D. E. *et al.* Identification of mouse AAV capsid-specific CD8+ T cell epitopes. *Mol. Ther.* **12**, 1023–33 (2005).
40. Wu, T.-L. *et al.* CD8+ T cell recognition of epitopes within the capsid of adeno-associated virus 8-based gene transfer vectors depends on vectors' genome. *Mol. Ther.* **22**, 42–51 (2014).
41. Madsen, D., Cantwell, E. R., O'Brien, T., Johnson, P. A. & Mahon, B. P. Adeno-associated virus serotype 2 induces cell-mediated immune responses directed against multiple epitopes of the capsid protein VP1. *J. Gen. Virol.* **90**, 2622–33 (2009).
42. Manno, C. S. *et al.* Successful transduction of liver in hemophilia by AAV-Factor IX and limitations imposed by the host immune response. *Nat. Med.* **12**, 342–7 (2006).
43. Sabatino, D. E. *et al.* Identification of mouse AAV capsid-specific CD8+ T cell epitopes. *Mol. Ther.* **12**, 1023–33 (2005).
44. Mingozzi, F. & High, K. A. Immune responses to AAV in clinical trials. *Curr. Gene Ther.* **7**, 316–24 (2007).
45. Mingozzi, F. *et al.* CD8(+) T-cell responses to adeno-associated virus capsid in humans. *Nat. Med.* **13**, 419–22 (2007).
46. Gao, G. *et al.* Clades of Adeno-Associated Viruses Are Widely Disseminated in Human Tissues Clades of Adeno-Associated Viruses Are Widely Disseminated in Human Tissues. (s2004). doi:10.1128/JVI.78.12.6381.

47. Grimm, D. *et al*. In vitro and in vivo gene therapy vector evolution via multispecies interbreeding and retargeting of adeno-associated viruses. *J. Virol.* **82**, 5887–911 (2008).
48. Inagaki, K. *et al*. Robust systemic transduction with AAV9 vectors in mice: efficient global cardiac gene transfer superior to that of AAV8. *Mol. Ther.* **14**, 45–53 (2006).
49. Limberis, M. P., Vandenberghe, L. H., Zhang, L., Pickles, R. J. & Wilson, J. M. Transduction efficiencies of novel AAV vectors in mouse airway epithelium in vivo and human ciliated airway epithelium in vitro. *Mol. Ther.* **17**, 294–301 (2009).
50. Gao, G.-P. *et al*. Novel adeno-associated viruses from rhesus monkeys as vectors for human gene therapy. *Proc. Natl. Acad. Sci. U. S. A.* **99**, 11854–9 (2002).

Acknowledgments

We thank Dr. Hughes Fausther-Bovendo for reviewing the manuscript. We thank Mrs. Kathy Frost for her assistance with the MIRAX MIDI scanner. The work in this paper was funded by the Public Health Agency of Canada.

Author contributions

The author(s) have made the following declarations about their contributions: Conceived and designed experiments: A.B., A.A. and G.P.K. Performed the experiments: A.B., A.C. and J.A. Performed the western blots: G.S. Analyzed the data: A.B. Made the virus vectors: A.B., A.C. and J.A. Wrote the paper: A.B. and G.P.K. Supervised the research: A.A. and G.P.K. All authors reviewed the manuscript.

Additional information

Supplementary information accompanies this paper at http://www.nature.com/scientificreports

Competing financial interests: The authors declare no competing financial interests.

How to cite this article: Bello, A. *et al*. Novel Adeno-associated Viruses Derived From Pig Tissues Transduce Most Major Organs in Mice. *Sci. Rep.* **4**, 6644; DOI:10.1038/srep06644 (2014).